Journal of Sound and Vibration (1997) **203**(2), 219–236

SURFACE IMPEDANCE CONTROL FOR SOUND ABSORPTION: DIRECT AND HYBRID PASSIVE/ ACTIVE STRATEGIES

M. Furstoss, D. Thenail and M. A. Galland

Laboratoire de Mécanique des Fluides et d'Acoustique UMR CNRS 5509, *Ecole Centrale de Lyon*, *BP* 163, 69131 *Ecully Cedex*, *France*

(*Received* 16 *May* 1996, *and in final form* 18 *November* 1996)

Some active impedance control experiments in an anechoic chamber are reported. Further active methods are developed for the design of locally controlled absorption liners in air, whose basic principles were described by Olson and May and subsequently investigated practically by Guicking and his colleagues at the beginning of the 80's. Two methods are described and tested. In the first, processing of the acoustic pressure and velocity information from close to the membrane of a control loudspeaker is used to produce a desired impedance. In the second active and passive means are combined: the impedance of the rear face of a porous layer is actively controlled so as to make the front face normal impedance take on a prescribed value. The impedance matching performance of both systems subject to an incident acoustic field including a single secondary loudspeaker is studied for both normal and oblique incidence. The combination of active and passive methods is a pragmatic approach, the aim of which is to simplify the control system for impedance control over extensive areas of wall. Indeed, the association of active control with a porous material allows the active system to be reduced in complexity to a simple active pressure release. Even though somewhat sub-optimal for sound absorption, the hybrid passive/active systems support feedback methods and lead to highly absorptive coatings.

1. INTRODUCTION

The original form of active noise control presented by Lueg [1] consisted of sound pressure reduction by the superposition of a secondary acoustic signal 180 degrees out of phase with the unwanted sound. About 20 years later, Olson and May carried out the first significant active control experiments and they also suggested a somewhat different active noise control method based on interference [2]: their "Electronic Sound Absorber" in which an electroacoustic feedback loop was used to drive the acoustic pressure to zero near an error microphone placed close to a secondary loudspeaker. As stated by these authors, they had designed a "sound pressure reducer". In their paper, however, the possibility of using the secondary loudspeaker to "absorb" sound was also considered. Then, placing the initial "spot type noise reducer" behind acoustically resistant cloth was suggested, the aim being to couple an acoustic resistance (having a correctly chosen value) with a low active impedance, so that the overall impedance "seen" by the incoming wave is approximately the cloth resistance, and thus acoustic dissipation by friction through the cloth is increased in the low frequency range. The use of active means for impedance control and absorption of sound was clearly presented.

0022–460X/97/220219 + 18 $25.00/0/sv960905

Active absorbing methods have been thereafter experimented by Guicking and colleagues [3–5]. Their initial experiments were conducted in an impedance tube terminated by a controlled loudspeaker [3]. An analogue control circuit, whose input was provided by a two microphone probe in order to avoid feedback instabilities, allowed arbitrary reflection coefficients between 0 and 1·5 for frequencies below 1000 Hz (impedance control could produce power absorption or overreflection). This method was later tested in an anechoic room [5]. A 3×3 loudspeaker array was used to control normally as well as obliquely incident plane waves. The reflection coefficient could be adjusted between about 10% and 200% for sinusoidal waves. However, near-field effects caused major accuracy problems and broadband experiments remained to be conducted. Beside the above work, which could be termed "direct impedance control", Guicking and Lorentz also studied the combination of a "spot type noise reducer" and an acoustically resistant cloth [4]. This system referred to the "active equivalent of the $\lambda/4$ resonance absorber", which is the conventional passive method for improving the acoustic absorption of porous layers.

More recently, the increasing interest in time adaptive feedforward methods [6] led to further works addressing impedance control in a one-dimensional system. Orduña–Bustamante and Nelson successfully constructed an active absorber for periodic, random and transient plane sound waves [7]. The "filtered-X" LMS algorithm processed the signals from two microphones in order to attain a desired acoustic impedance at the termination for frequencies below 1000 Hz. For the same purpose, Nicholson and Darlington [8], and Thenail and Galland [9] developed systems which control the secondary loudspeaker surface impedance by processing its membrane velocity and the pressure in its vicinity by using similar algorithms.

It is worth mentioning, in this non-exhaustive overview of experiments, other applications concerned with underwater acoustics and ultrasonic propagation. The ability to cancel reflected waves on a surface was studied for different water filled guides terminated by an active coating. Piezoelectric polymers were generally used both as sensors and actuators, which simultaneously cancelled reflection and transmission of normally incident waves (by Howarth *et al*. [10, 11]). In the field of ultrasonic propagation, extended planar active surfaces able to absorb obliquely incident plane airborne waves have been also constructed by Ruppel and Shields [12].

Beside these various set-ups effectively achieving active impedance changes, the relevance of active sound absorption for noise reduction itself has been long the subject of important research [6, 13, 14]. Nelson and Elliott, among other contributions [15], considered a "global control" strategy for noise abatement: the total acoustic energy in an enclosure or the total power output of a source array in the free field are cost functions to be minimized. They demonstrated that maximum absorption of sound can be a suboptimal strategy (although useful to reduce sound levels at the enclosure's acoustic resonances). This result was obtained from an essentially feedforward control principle: i.e., one operates at a single frequency and assumes the availability of a reliable reference signal at the same frequency. An alternative feedback approach has been more recently adopted by Clark and colleagues [16, 17]. The acoustic application of direct rate feedback control allows an added active damping, which dissipates energy and guarantees stability margins. In the following work, active impedance control is considered in the context of sound absorption. Feedback control underlies the overall project although many experiments presented herein use feedforward methods for the sake of feasibility checks.

Two methods which the authors previously tested in an impedance tube [9, 19] are used. The present experiments were performed in an anechoic chamber and test the system's behaviour under normal and oblique incidence, at frequencies below 1000 Hz. The first system studied involves direct control of the acoustic impedance of a loudspeaker, via the

simultaneous processing of the membrane velocity and the acoustic pressure in its close vicinity by a feedforward technique. The second method controls the impedance at the rear face of a porous layer, in order to drive the front face impedance to a prescribed value. Besides the possibility of assigning some desired impedance value to a porous material surface, this set-up allows one to investigate further, experimentally, the "active equivalent of the $\lambda/4$ resonance absorber" of Olson and May [2] as a system which maximizes the low frequency absorption of a thin material sample. The active system is greatly simplified by pressure minimization at the rear face of a thin porous material layer. The influence of this rear face condition on the material absorption is studied both for normal and oblique incidence. A feedback experiment involving a 3×3 loudspeakers array demonstrates the potential of the method for realistic noise control problems.

2. DIRECT IMPEDANCE CONTROL

This section deals with the direct control of normal surface impedance by the simultaneous processing of both acoustic pressure and normal velocity measurements. First, the output that the controller must produce is determined by considering the case of an infinite impedance plane with incident plane waves; the elements of the control system and the overall experimental facilities are also presented. Next, the results of impedance control under normal and oblique incidence are described.

2.1. PRINCIPLE AND EXPERIMENTAL SET-UP

The simple case of an infinite plane (S) set in a free field with incident plane waves with an angle of incidence θ is considered (See Figure 1). The determination of the impedance which cancels any reflection at the surface is straightforward. The reflection coefficient R can be written as a function of the surface impedance Z:

$$R = (Z - Z_0/\cos\theta)/(Z + Z_0/\cos\theta). \tag{1}$$

$Z_0 = \rho_0 c_0$ is the characteristic acoustic impedance, c_0 the sound speed, and ρ_0 the air density. Here we leave aside the case of grazing incidence. Since the intention is to cause the reflected wave from (S) to vanish, the impedance has to be $Z = Z_0/\cos\theta$ in the oblique incidence case ($Z = Z_0$ in the normal incidence case).

The experimental set-up is depicted in Figure 2. The impedance plane is a 10 cm square flat membrane of a loudspeaker (ref: HDP15, manufactured by Audax Inc.). In the context of the wavelengths of concern, the actual magnitude of the impedance makes the use of formula (1) *a priori* suspect. The extent to which the diffraction effects of the surroundings contribute to the acoustic field above an absorbent material panel and disturb impedance measurements has been investigated by Allard and Delage [20]. They simulated, via an integral formulation, the reflection from a surface of given impedance and attempted to find this value experimentally by scanning the acoustic field above, in

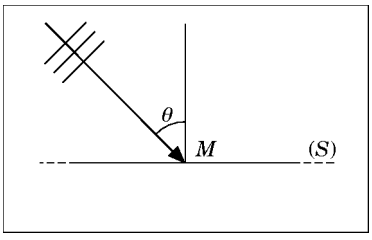

Figure 1. Plane waves impinging on a surface of impedance Z.

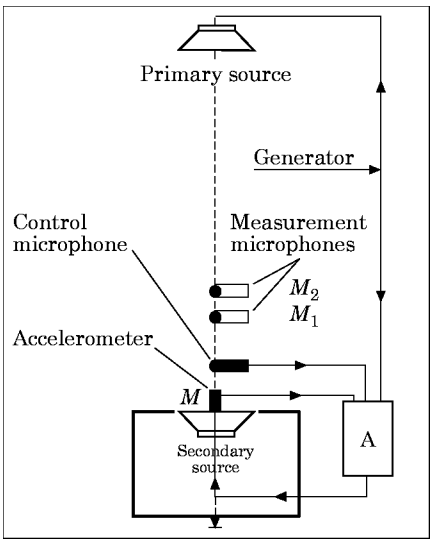

Figure 2. Direct impedance control using a flat loudspeaker membrane. A is the controller.

the same way as in a Kundt interferometer. They found the best agreement in the case of the most absorbent surface. Further numerical results mentioned in reference [21] involved a two microphone probe set close to the center of an impedance panel. The confidence in measurements (and in expression (1) in the context of our work) was seen to extend to wider ranges of acoustic wavelengths to panel size ratios. The present active control set-up, the description of which follows next, provides the experimental version of the above numerical check, the agreement between measured and desired impedances demonstrating the effectiveness of both active impedance control and impedance measurement procedure.

The normal impedance at the controlled surface is measured by using a method which was developed by Allard and Sieben at low frequencies in the normal incidence case [21] and extended to the oblique incidence case [22]. This measurement procedure can also be viewed as the extension of a method developed by Chung and Blaser for the determination of the surface impedance of materials in an impedance tube [23]. At a sufficient distance from the primary noise source, the plane wave hypothesis remains valid in a free field. A probe, which consists of two microphones aligned normally with the surface, provides the impedance at the mid-point between the two microphones according to

$$Z_p(\omega) = \mathrm{j}\omega\rho_0\Delta r[1 + H_{12}(\mathrm{j}\omega)]/2[H_{12}(\mathrm{j}\omega) - 1], \tag{2}$$

where Δr is the distance between the microphones M_1 and M_2, and $H_{12}(\mathrm{j}\omega)$ is the frequency response function relating the output signals of the microphones M_1 and M_2; the time dependence $e^{j\omega t}$ is assumed. The probe is set very close to the controlled surface (a few centimeters), leading also to negligible losses along the distance s between M and the impedance plane. The surface impedance is then expressed as

$$Z(\omega) = Z_0\,[\mathrm{j}Z_p(\omega)\,\mathrm{cotan}\,(k_0 s) + Z_0]/[Z_p(\omega) + \mathrm{j}Z_0\,\mathrm{cotan}\,(k_0 s)]. \tag{3}$$

One of the advantages of this method is that it allows measurements of reasonably (dictated by Δr) broadband noise. The phase and amplitude mismatches between the two sensors are corrected by relative calibration.

The primary acoustic field is created by an unbaffled loudspeaker set about 1·2 m above the active system. Its dipole nature induces a higher signal at the controlled surface, and a lower one around its perimeter, where diffraction effects are generated. The experimental set-up depicted in Figure 2 was used for normal and oblique incident waves. This work was undertaken in an anechoic chamber in the Fluid Mechanics and Acoustics Laboratory at the Ecole Centrale de Lyon. The chamber has dimensions 6·1 m × 4·6 m × 3·8 m and a cut-off frequency of approximately 100 Hz.

2.2. THE CONTROL PROCEDURE

An accelerometer is fixed on the controlled surface (the secondary loudspeaker membrane) and a microphone is placed nearby. The controller is a digital filter and its hardware, which includes an Analog Devices ADSP 2101 digital signal microprocessor, allows the implementation of time adaptive algorithms. Optimal signal processing performance is attained because the reference signal is the electric signal that serves as input for the primary noise source, allowing one to avoid feedback instability. The pressure and velocity signals provided by the microphone and the accelerometer are converted into digital form, and processed in order to synthesize at every sample time the error signal given by

$$\varepsilon = p - Zv, \tag{4}$$

where Z takes on a real value and does not depend on frequency; it is set by the controller's user before starting the overall control procedure. Then, the filter coefficients are adjusted by the microprocessor in order to minimize the error signal power in the least squares sense via the "filtered-X" LMS algorithm [6]. The filtered reference signal is generated by passing the controller's input through an estimate of the error path response $H(j\omega) - ZG(j\omega)$, the frequency response functions $H(j\omega)$ and $G(j\omega)$ between the loudspeaker input and the sensors' (microphone and accelerometer, respectively) outputs being measured prior to control.

2.3. IMPEDANCE CONTROL UNDER NORMAL INCIDENCE

The desired impedance value at the loudspeaker surface is $Z = Z_0$. The primary noise disturbance is broadband normally incident noise over the frequency range 150–500 Hz. Figure 3 shows the real and imaginary parts of the reduced impedance $\zeta = Z/Z_0$, which is measured by the two-microphone probe with control. Despite the surroundings' diffraction effects and other potential errors (in particular, transduction errors, as also considered by Darlington *et al*. [24]), the agreement between the expected unity value and the measured impedance appears fairly good down to about 150 Hz. The absorption coefficient which results from the impedance measurement is shown in Figure 4. Its value

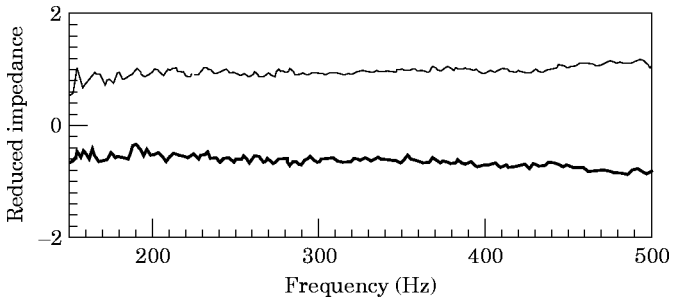

Figure 3. Real (——) and imaginary (▬) parts of the measured normal reduced impedance.

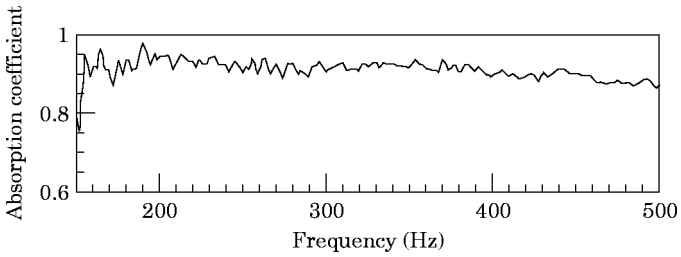

Figure 4. Absorption coefficient of the controlled surface under normal incidence.

remains close to 1 over the control frequency range, and thus the system absorbs nearly all incident acoustic waves.

The performance of the system investigated has been shown in the close vicinity of the center of the active surface. Now, the microphone probe position is changed and varies along a horizontal axis above the membrane for a single frequency of excitation. The graph of the absorption coefficient which is shown in Figure 5 indicates that the impedance control is effective over the whole loudspeaker membrane.

2.4. IMPEDANCE CONTROL UNDER OBLIQUE INCIDENCE

In this section, the performance of the system is described for oblique incident plane waves. In the following, the results for the incidence angle $\theta = 60^\circ$ are reported since it seems to be the largest value at which the impedance measurement method remains valid, according to observations given in reference [25]. The prescribed impedance value is $Z_0/\cos\theta$. For convenience in the observation of the measurements, it has been chosen to normalize the measured impedance by $Z_0/\cos\theta$ so that it is still to be compared with unity. The variations of the real and imaginary parts of the measured impedance are presented in Figure 6 and the absorption coefficient in Figure 7. In the oblique incidence case, diffraction due to the overall environment and especially to the loudspeaker enclosure were expected greatly to distort the acoustic field at the probe location. However, the measured impedance is still seen to be very close to the value the active control aims to assign. Another experiment, which has not been reported here, has been undertaken at 45°. It

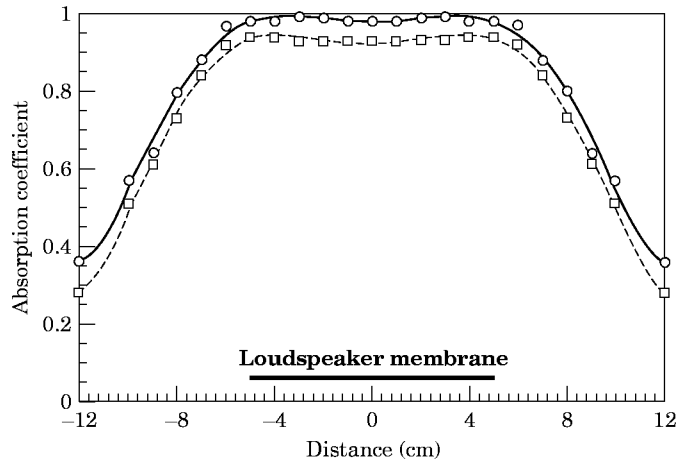

Figure 5. Absorption coefficient above the loudspeaker membrane under normal incidence. The assigned impedance value is $Z_0 = \rho_0 c_0$. Measured values: ○, 200 Hz; □; 400 Hz.

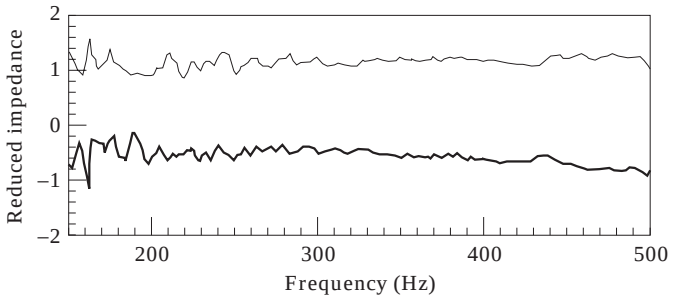

Figure 6. Variation of the real (——) and imaginary (▬) parts of the measured impedance with $\theta = 60^\circ$ incidence. The assigned impedance value is $Z_0/\cos\theta$. The measurements are normalized by $Z_0/\cos\theta$.

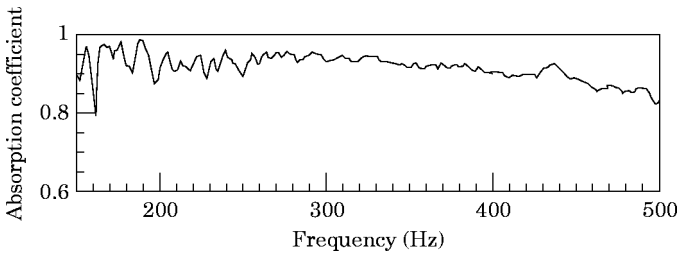

Figure 7. Variation of the absorption coefficient with $\theta = 60^\circ$ incidence. The assigned impedance value is $Z_0/\cos\theta$.

provided results similar to the ones shown here for 60°, and further measurements also showed that the region of very high absorption extends over the whole active surface of the loudspeaker. Thus, the three cases $\theta = 0$, 45, and 60° strongly suggest the effectiveness of active control in establishing a specified impedance for any oblique incidence up to 60°.

2.5. THEORETICAL AND PRACTICAL LIMITATIONS

There is a need for practical compromises in the implementation of active absorbers for realistic environments, owing to the limitations that are now outlined.

First, the discussion above is for a well defined incidence angle, but a practical active absorber is expected to be placed in situations in which neither the number nor the positions of the sources are determined *a priori*. In what follows, attention is restricted to the design of an active liner which assigns the impedance Z_0 appropriate to normal incidence. As can be seen from Figure 8, the absorption coefficient for a 60° incidence is about 0·9 over the whole frequency range, in accordance with equation (1). The achieved active surface of normal impedance Z_0 is absorbent for a wide range of incident angles.

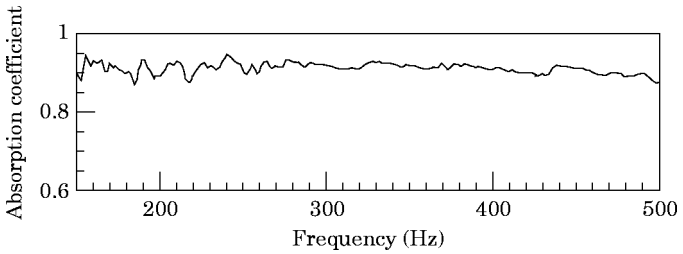

Figure 8. Variation of the absorption coefficient with 60° incidence. The assigned impedance value is Z_0.

On the other hand, the signal processing which has been employed above is not suited for a lot of noise control problems. Indeed, a reliable prior knowledge of the undesirable primary signal is not always at one's disposal, and it is likely that this feedforward technique will be confined to some specific applications. Efforts to implement feedback techniques were not so conclusive for broadband excitations.

A further complication is that the accelerometer inertia changes the loudspeaker response and consequently the frequency bandwidth is limited. In the present case, impedance assignment is no longer possible for frequencies higher than about 600 Hz.

Finally, the assignment of a desired impedance, Z, at a surface requires accurately calibrated pressure and velocity sensors. This would make application of the technique to extensive surfaces expensive.

The method which is investigated in the next section and which is aimed at resolving these problems, at least in part, is to combine a porous layer with an active system.

3. ACTIVE IMPEDANCE CONTROL FOR INCREASED ABSORPTION BY A POROUS LAYER

In this section, a second impedance control system, which exploits the characteristics of a porous layer in addition to active control is considered. The basis is the $\lambda/4$ resonance absorber, which is described first. Since the design exploits the behaviour of porous materials at low frequencies, attention is also paid to the validity of the method as frequency increases. Experiments are then reported and indicate that this combined active/passive method works well and is suited to practical implementation and development.

3.1. THE $\lambda/4$ RESONANCE ABSORBER

Absorption by a porous layer, such as fibreglass, depends not only on the layer, but also on its acoustic environment. In particular, the layer backing is important. Clearly, a relatively thin porous material layer is inefficient at low frequencies when it is supported by a motionless, impervious surface. The problem to increase the absorption is to act so that the material acoustic properties, which are "seen" by the incoming wave, are significantly different to that of the rigid impervious support. For instance, an air gap between the rear face and an impervious, rigid surface generally improves low frequency absorption, as explained below.

At low frequencies, viscous forces in a porous material predominate over inertial ones and the acoustic behaviour is mainly described by the flow resistivity, whose meaning is given in Figure 9. A steady pressure drop $\Delta P = P_2 - P_1$ across a porous layer of thickness d induces a steady flow of air V, and the flow resistivity is

$$\sigma = \Delta P / V d. \tag{5}$$

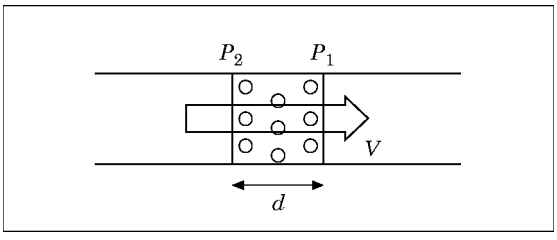

Figure 9. A porous layer of thickness d in a steady flow of air speed V.

(It is assumed that V is sufficiently small that σ is a constant). From the above equation and referenced figure, the low frequency asymptotic behaviour is described by:

$$\sigma d = (p_2 - p_1)/v, \tag{6}$$

where p_1, p_2 and v are now acoustic quantities. Thus, if the porous layer is placed at a quarter of wavelength from a rigid impervious surface, the back pressure vanishes and the layer input impedance can be approximated by the flow resistance:

$$p_2/v = \sigma d. \tag{7}$$

Consequently, a good low frequency absorber (often called a $\lambda/4$ resonance absorber) results from a suitable material thickness (whose flow resistance equals the air impedance Z_0). The idea which was first proposed by Olson and May [2] is to maintain a low impedance at the back face by using an active control system. This method was experimentally investigated in an impedance tube by Guicking and Lorentz [4], who also pointed out the advantages of the active control solution, as compared to the conventional passive $\lambda/4$ absorber. The active control system avoids the bulky air gap of the passive resonance absorber at low frequency. Furthermore, it presents a broadband efficiency whereas the frequency bandwidths of increased absorption are narrow for a passive resonance absorber including a thin porous material layer. Since then, the hybrid active/passive design has been exploited by the present authors using modern electronics and signal processing up to frequencies which are no longer "low" [19]. In this case, the acoustic short circuit at the rear face of a $\rho_0 c_0$ layer no longer provides anechoism at the layer front face, and hence, two questions arise when both frequency and incidence are allowed to vary: what condition should be assigned at the rear face to achieve perfect matching between the layer input impedance and that of the incident acoustic field, and to what extent system performance decreases if, instead of the ideal condition, pressure release is used.

3.2. ACTIVE CONTROL OF THE SURFACE IMPEDANCE OF A FIBREGLASS LAYER FOR NORMAL OR OBLIQUE INCIDENCE PLANE WAVES

A previous study, similar to what follows, has already been reported for the one-dimensional case of the impedance tube by two of the authors [18]. The model used for the description of the acoustic behaviour of a porous medium is described in a recent book by Allard [26].

3.2.1. *Theory*

The aim of this section is to determine the impedance to be assigned at the rear face of a porous layer, so that no reflection occurs at the front face. The problem is illustrated by Figure 10: a porous material layer is backed by a plane of impedance Z, its front face exposed to an acoustic plane wave of incidence θ.

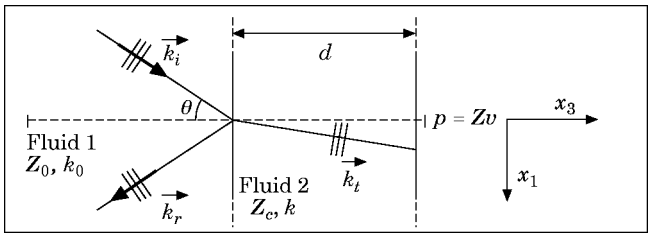

Figure 10. Isotropic porous material backed by an impedance plane under oblique incidence.

One initially supposes that the layer material is homogeneous and isotropic. Its rigid frame is assumed to be motionless, so that the porous layer can be replaced by an equivalent viscothermal fluid. It may also be noted that the active control of the surface impedance of a porous layer whose solid frame vibrates significantly is also theoretically possible (see the report by Bolton and Green [27]).

In the present model, viscous and inertial effects on the one hand, and thermal exchanges between the rigid frame and the saturating fluid on the other, are treated separately. Viscous and inertial effects inside the porous medium are taken into account via a complex dynamic density $\rho(\omega)$. Thermal exchanges between the fluid and solid phases are described by a complex dynamic bulk modulus $K(\omega)$. For the two-dimensional case depicted in Figure 10, the pressure satisfies the equation

$$(\nabla^2 + k(\omega)^2)p(x_1, x_3) = 0, \tag{8}$$

where ∇^2 is the Laplacian operator and $k(\omega)$ is the wave number of the equivalent fluid given by

$$k(\omega) = \omega\{\rho(\omega)/K(\omega)\}^{1/2}, \tag{9}$$

while the complex characteristic impedance is

$$Z_c(\omega) = \{\rho(\omega)K(\omega)\}^{1/2}. \tag{10}$$

The expression for the dynamic density was suggested by Johnson *et al*. [28], while that for the dynamic bulk modulus was given by Champoux and Allard [29]. Five parameters are required for a general rigid framed porous medium, but in the particular case of a fibrous highly porous material, Allard and Champoux [30] derived relations which express the dynamic density and bulk modulus as a function of a single parameter: the flow resistivity σ, which appears via another parameter $X = \rho_0 f/\sigma (f = \omega/(2\pi))$. Thus

$$\rho(\omega) = 1{\cdot}2 + (-0{\cdot}0364X^{-2} - \mathrm{i}0{\cdot}1144X^{-1})^{1/2}, \tag{11}$$

$$K(\omega) = 101320\,\frac{\mathrm{i}29{\cdot}64 + (2{\cdot}82X^{-2} + \mathrm{i}24{\cdot}9X^{-1})^{1/2}}{\mathrm{i}21{\cdot}17 + (2{\cdot}82X^{-2} + \mathrm{i}24{\cdot}9X^{-1})^{1/2}}. \tag{12}$$

The back face impedance, Z, is now written as a function of the front face surface impedance Z_s. At any given angular frequency ω, Z is given by

$$Z = \frac{Z_c k}{k_{t3}}\,\frac{\mathrm{j}Z_s \operatorname{cotan}(k_{t3}d) + Z_c k/k_{t3}}{Z_s + \mathrm{j}Z_c(k/k_{t3})\operatorname{cotan}(k_{t3}d)} \tag{13}$$

In expression (13), k_{t3} is the $\vec{k}_t$ component along the x_3 axis (see Figure 10), and is given by

$$k_{t3} = (k^2 - k_0^2 \sin^2\theta)^{1/2}. \tag{14}$$

The optimal back impedance Z_{opt}, which corresponds to the total absorption of sound, is deduced from equation (13) or by letting $Z_s = Z_0/\cos\theta$. Figures 11 and 12 show the real and imaginary parts of $\zeta_{opt} (= Z_{opt}/Z_0)$ for two material samples of thicknesses 2 and 7 cm, the frequency increasing from 0–20 kHz along each curve. The flow resistivity, σ, is 20 000 Rayls/m, approximately that of the fibreglass used in the present experiments (manufactured by Marmonier S.A.) according to a best fit with experimental impedance measurements when the material is attached to a rigid wall. Figure 11 shows the normal incidence case, and Figure 12, the case of an incidence of 45°.

The normal incidence case is considered first. The 2 cm thick fibreglass layer makes the flow resistance of the layer $\sigma d = 400$ Rayls, approximately the air impedance. The low

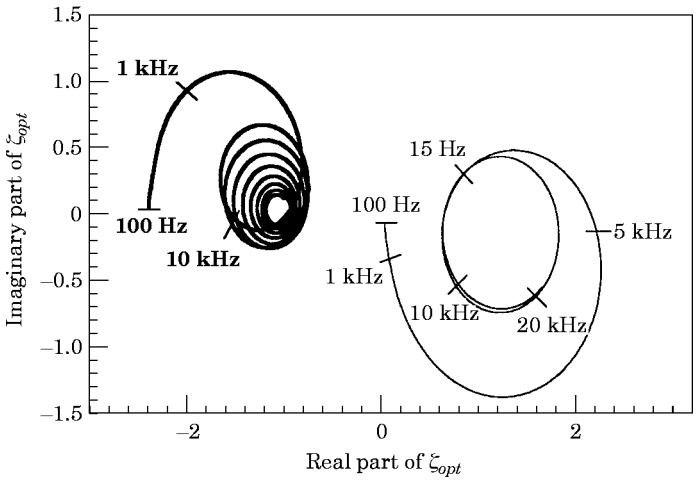

Figure 11. Optimal back face impedance of two material samples in air under normal incidence $\sigma = 20\,000$ Rayls/m. ▬, $d = 7$ cm; ——, $d = 2$ cm.

frequency limit of the spiral shown in Figure 11 is very close to $\zeta_{opt} = 0$ and corresponds to the resonance absorber. It is also seen that the optimal impedance for the layer rear face remains close to zero over the frequency range 0–1000 Hz; that is, over most of the band of poor absorption of an equivalent hard backed layer. Thus, pressure release at the layer rear face is seen to remain a desirable objective over the whole range 0–1000 Hz. The second spiral in Figure 11 shows the variation of ζ_{opt} for a 7 cm thick layer.

As previously stated in reference [18], very different energetics can be observed at the controlled impedance plane. The real part of ζ_{opt} is always positive when $d = 2$ cm, so that the impedance plane absorbs power. In the 7 cm case, the real part of ζ_{opt} is always negative and the impedance plane has to supply power. When the layer is thicker, the backing boundary condition is seen less by an incident wave and the controlled plane has to supply power if an effect is to be observed at the front face of the layer.

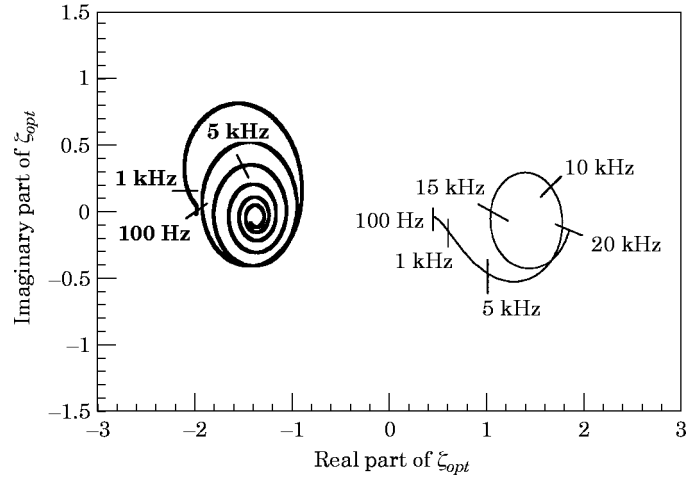

Figure 12. Optimal back face impedance of two material samples in air under oblique incidence (45°). Key as Figure 11.

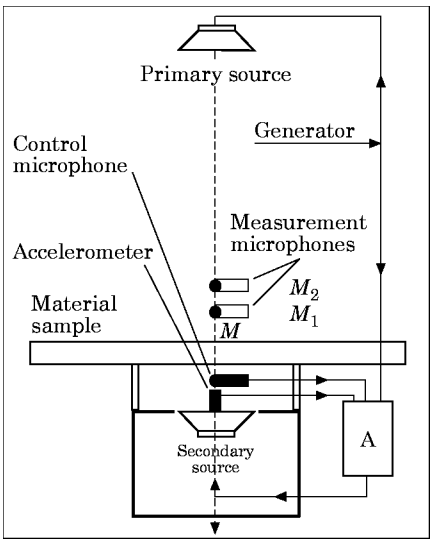

Figure 13. Experimental set-up.

The case of 45° incidence is presented in Figure 12. The reduced impedance required at the layer front face is then $\zeta = 1/\cos\theta\ (=\sqrt{2})$. Application of the pressure release $\zeta = 0$ at the rear face is then appropriate at low frequencies if the layer resistance is $\sigma d = Z_0/\cos\theta$.

3.2.2. *Experimental set-up*

In order to observe experimentally some of the results of the above theoretical analysis, the set-up of the previous section was used to control the impedance at the back of a fibreglass panel. A 1 m^2 square, 2 cm thick panel is set above the controlled impedance plane, as shown in Figure 13. The sensing and signal processing devices used in this section (feedforward control method and impedance measurements procedure) have already been presented. The controller aims to assign purely real impedances for a chosen excitation frequency of 300 Hz.

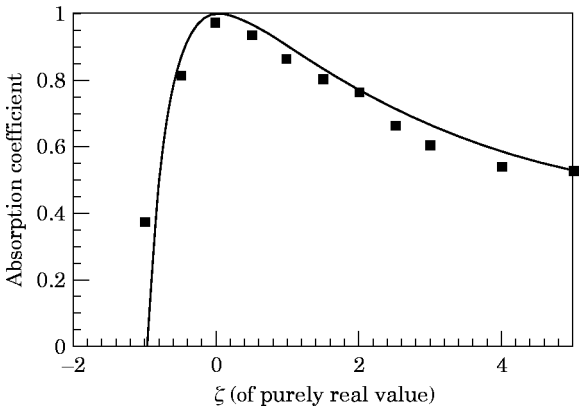

Figure 14. Variation under normal incidence of the absorption coefficient of a fibreglass panel ($d = 2$ cm, $f = 300$ Hz) with its back face impedance imposed by the control system. ■, Measurements; ——, model.

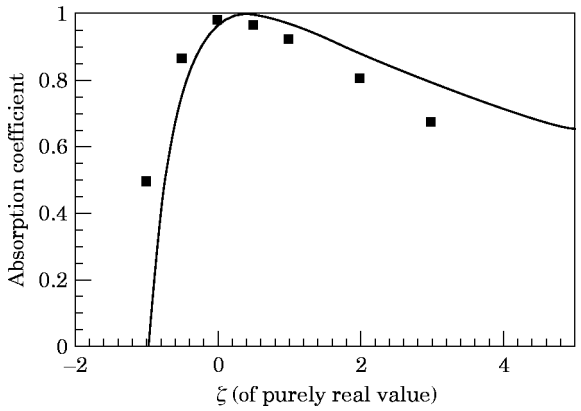

Figure 15. Variation under (45°) incidence of the absorption coefficient of a fibreglass panel ($d = 2$ cm, $f = 300$ Hz) with its back face impedance imposed by the control system. Key as figure 14.

The results for the normal incidence case are presented in Figure 14. For each of the rear face impedances assigned by the controller, excellent agreement is obtained between the measured front face impedance and that predicted by using the relations of Allard and Champoux. The results obtained for the 45° incidence case are shown in Figure 15. The agreement between measured and predicted front face impedances remains good. These experiments further confirm the relevance of a pressure release at the panel back face, and the reliance in the "active equivalent of the $\lambda/4$ resonance absorber".

Note that the good accuracy of these experiments suggests that impedance control might be an interesting tool for a refined characterization of acoustic propagation in porous media. Indeed, their dynamic density $\rho(\omega)$ and bulk modulus $K(\omega)$ may be determined from front face impedance measurements while different impedances are actively assigned at the back face. The subject is under current investigations.

3.3. IMPROVED ABSORPTION BY A FIBREGLASS SAMPLE BY USING PRESSURE MINIMIZATION AT ITS REAR FACE

In the following experiments, the pressure at the rear face of a fibreglass panel is actively driven to zero. Normal and oblique incidence cases are successively considered. The resulting impedance is measured; attention is also paid to the area dimensions of increased absorption.

The experimental set-up is the same as depicted in Figure 13, with a single electret microphone, as control sensor. It is set some millimeters from the material rear face (the panel used in section 3.2.). The secondary loudspeaker has a circular membrane of diameter 20 cm. Control has been achieved via the feedforward method described in previous sections. The excitation frequency range of the primary source is 200–900 Hz. The attenuation at the control microphone is about 25 dB over the whole frequency range.

The impedance and absorption curves in the normal incidence case are presented in Figures 16 and 17 respectively. The impedance at the material front face is seen to be approximately equal to that of air, Z_0. In Figure 17, the absorption coefficient of the same material sample with a rigid backing is also shown for comparison: absorption is increased in a very important manner over the whole frequency range.

The benefits for absorption may also be evaluated as a function of the radial distance, r, on the panel front face from the center of the loudspeaker. Figure 17 also shows the variations of the absorption coefficient with the frequency at the limit of the membrane ($r = 10$ cm). Although acoustic pressure at the panel rear face is less attenuated (8 dB

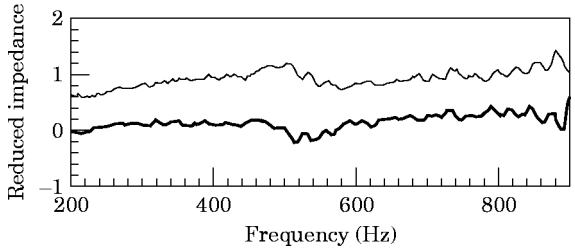

Figure 16. Reduced impedance of the fibreglass panel, when backed by zero pressure under normal incidence. ——, Real part; ▬▬, imaginary part.

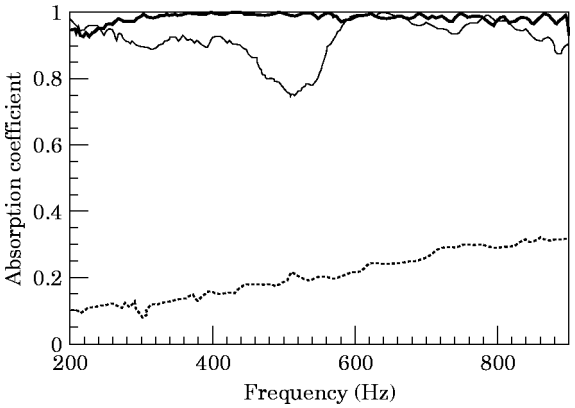

Figure 17. Absorption coefficient of the fibreglass panel when backed by a zero pressure under normal incidence. The microphone probe is successively set on the vertical axis ($r = 0$) (——), and at 10 cm from the vertical axis ($r = 10$ cm) (▬▬). · · · · Denotes the absorption coefficient when the material is rigidly backed.

instead of 25 dB at $r = 0$), the absorption coefficient nonetheless remains large. Figure 18 shows the variations of the absorption coefficient at 400 Hz with the radial position, r. The benefits for absorption are very significant over the whole surface of the fibreglass above the loudspeaker membrane.

The system has also been tested for both 45° and 60° incidence waves, and the results are shown in Figure 19. In both cases, the pressure release departs significantly from the low frequency optimal impedance. Nevertheless, important benefits in the absorption

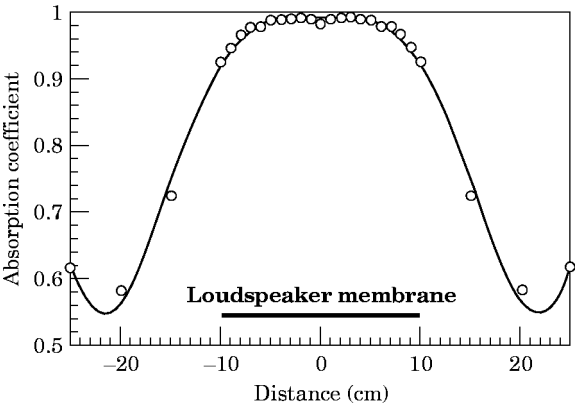

Figure 18. Plot of the absorption coefficient as a function of r, under normal incidence for $f = 400$ Hz. ○, Measured values; ——, fitted curve.

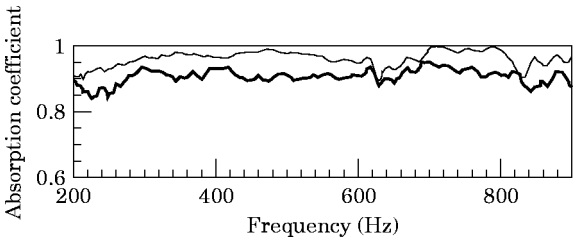

Figure 19. Absorption coefficient of the fibreglass panel backed by a zero pressure for 45° (——) and 60° (▬) incidence.

coefficient are observed up to 60° incidence over the whole frequency range. As in the normal incidence case, measurements were also performed at different r. Again, the effect is uniform over the whole surface above the membrane.

Compared to the impedance control system presented in section 2, the hybrid active/passive absorber produces high absorption over wider frequency ranges, and its design is more simple. The last experiment we will present involves relatively simple feedback filters controlling multicells independent systems, thus showing the feasibility in constructing larger active absorbent linings.

3.4. FEED-BACK CONTROL EXPERIMENTS WITH A 3 × 3 LOUDSPEAKERS ARRAY

Larger active anechoic surfaces design requires a secondary sources amount which is dictated by the wavelengths of concern. The same fibreglass panel is backed by a 3 × 3 loudspeakers array. Each individual secondary source is controlled by a relatively simple feedback controller, an analogue filter whose transfer function exhibits two poles and two zeros. This controller, which is commonly implemented in active anti-noise headsets [31], cancels the acoustic pressure at the fibreglass back face. Feedback instabilities, however, has limited to 200–400 Hz the frequency range of increased absorption. Measurements are performed at the material surface along an horizontal axis above three loudspeakers. Normal and 45° incidence results are given in Figures 20 and 21, respectively. Same performance is measured above each loudspeaker and the whole surface is seen to be highly

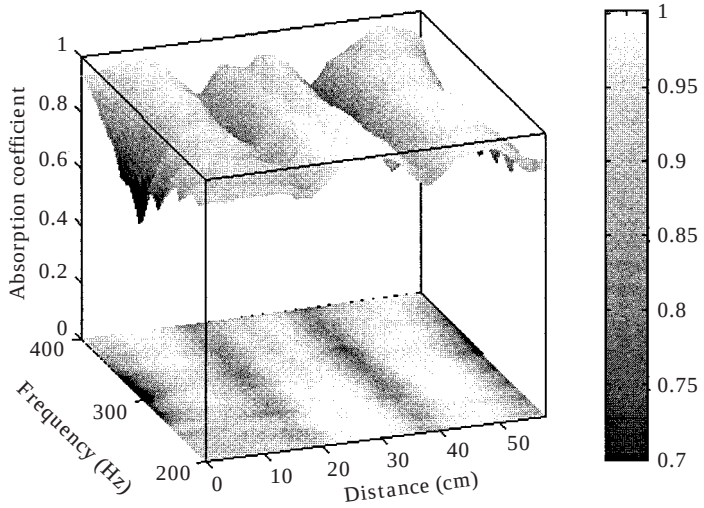

Figure 20. Absorption coefficient of the fibreglass panel backed by a 3 × 3 loudspeakers array under normal incidence.

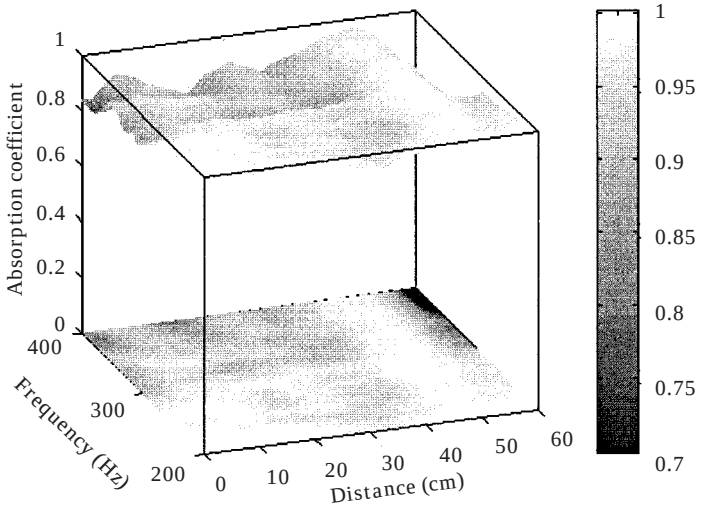

Figure 21. Absorption coefficient of the fibreglass panel backed by a 3×3 loudspeakers array under 45° incidence.

absorbent. Further work must include faster transduction devices, in order to shift the attainable high frequency limit, at least to reach the frequency range of good absorption by conventional passive porous layers.

4. CONCLUSIONS

Two different active systems for controlling a surface normal impedance have been presented and tested in an anechoic chamber. Direct impedance control simultaneously processes the acoustic pressure and velocity near a loudspeaker membrane which is driven by the controller in order to assign a prescribed impedance value for both normal and oblique plane waves. Reflected waves are cancelled over the 150–500 Hz frequency wave.

In the second impedance control procedure active control of the impedance at the rear face of a porous material panel is used, so that the front face impedance takes on a desired value. In this work, particular attention has been paid to the "active equivalent of the $\lambda/4$ resonance absorber". It results as the low frequency limit of porous material behaviour, but pressure release at the back face of an appropriately chosen porous panel produces high absorption over wide ranges of frequency and incidence angle. Relatively simple feedback approaches can be applied for that purpose when unwanted noise is unexpected and reasonably broadband. In addition, the controlled region (behind the porous layer) is separated from the incident acoustic field, an important advantage when there is perturbation by air flows. In sum, very promising features are given by this hybrid active/passive method.

ACKNOWLEDGMENTS

The authors express their gratitude to Professor J. Scott (Ecole Centrale de Lyon, France) and Professor A. J. Brammer (National Research Council, Canada) for many comments and discussions. D. Thenail is currently post-doctoral fellow of the Centre National d'Etudes Spatiales.

REFERENCES

1. P. Lueg 1936 *US Patent*, 2043416. Process of silencing sound oscillations.
2. H. F. Olson and E. G. May 1953 *Journal of the Acoustical Society of America* **25**, 1130–1136. Electronic sound absorber.
3. D. Guicking and K. Karcher 1984 *ASME Journal of Vibration Acoustics*, *Stress Reliability and Design* **106**, 393–396. Active impedance control for one-dimensional sound.
4. D. Guicking and E. Lorentz 1984 *ASME Journal of Vibration Acoustics*, *Stress Reliability and Design* **106**, 389–392. An active sound absorber with porous plate.
5. D. Guicking, K. Karcher and M. Rollwage 1985 *Journal of the Acoustical Society of America* **78**, 1426–1434. Coherent active methods for applications in rooms acoustics.
6. P. A. Nelson and S. J. Elliott 1992 *Active Control of Sound*. London: Academic Press.
7. F. Orduña Bustamante and P. A. Nelson 1992 *Journal of the Acoustical Society of America* **91**, 2740–2747. An adaptive controller for the active absorption of sound.
8. G. C. Nicholson and P. Darlington 1991 *Proceedings of the Institute of Acoustics* **13**, 155–164. Smart surfaces for building acoustics.
9. D. Thenail and M. A. Galland 1992 *Proceedings Idee-Force EUR'ACOUSTICS*, *W*4, *Ecole Centrale de Lyon*. Development of an active anechoidal boundary.
10. T. R. Howarth, V. K. Varadan, X. Bao and V. V. Varadan 1992 *Journal of the Acoustical Society of America* **91**, 823–831. Piezocomposite coating for active underwater sound reduction.
11. T. R. Howarth, X. Bao, R. Moser, V. K. Varadan and V. V. Varadan 1993 *Journal of the Acoustical Society of America* **93**, 1613–1619. Digital time delay network for an active underwater acoustic coating.
12. T. H. Ruppel and F. D. Shields 1993 *Journal of the Acoustical Society of America* **93**, 1970–1977. Cancellation of air-borne acoustic plane waves obliquely incident upon a planar phased array of active surface elements.
13. M. J. M. Jessel and G. A. Mangiante 1972 *Journal of Sound and Vibration* **23**, 383–390. Active sound absorbers in an air duct.
14. J. E. Ffowcs Williams 1984 *Proceedings of the Royal Society of London* **395** A. Anti-Sound.
15. S. J. Elliott, P. Joseph, P. A. Nelson and M. E. Johnson 1991 *Journal of the Acoustical Society of America* **90**, 2501–2512. Power output minimization and power absorption in the active control of sound.
16. R. L. Clark and D. G. Cole 1995 *Journal of the Acoustical Society of America* **97**, 1710–1716. Active damping of enclosed sound fields through direct rate feedback control.
17. R. L. Clark, K. D. Frampton and D. G. Cole 1996 *Journal of Sound and Vibration* **195**, 701–718. Phase compensation for feedback control of enclosed sound fields.
18. D. Thenail, M. A. Galland, M. Sunyach and J. E. Ffowcs Williams 1994 *Comptes Rendus de l'Académie des Sciences Paris* **t. 318**, 37–41. Actively optimised anechoic surfaces.
19. D. Thenail, M. A. Galland, M. Furstoss and M. Sunyach 1994 *Proceedings of the* 1994 *ASME Winter Annual Meeting*, *Chicago IL DE*-75, *AM*-16*D*, 441–448. Absorption by an actively enhanced material.
20. J. F. Allard and P. Delage 1985 *Journal of Sound and Vibration* **101**, 161–170. Free-field measurements of absorption coefficients on square panels of absorbing materials.
21. J. F. Allard and B. Sieben 1985 *Journal of the Acoustical Society of America* **77**, 1617–1618. Measurements of acoustic impedance in a free field with two microphones and a spectrum analyser.
22. J. F. Allard, R. Bourdier and A. M. Bruneau 1985 *Journal of Sound and Vibration* **101**, 130–132. The measurement of acoustic impedance at oblique incidence with two microphones.
23. J. Y. Chung and D. A. Blaser 1980 *Journal of the Acoustical Society of America* **68**, 907–913. Transfert function method of measuring in-duct acoustic properties. i.theory. ii.experiment.
24. P. Darlington, G. C. Nicholson and S. E. Mercy 1995 *Acta Acustica* **3**, 345–349. Input transduction errors in active acoustic absorbers.
25. B. Brouard, D. Lafarge and J. F. Allard 1985 *Proceedings of the* 15*th International Congress on Acoustics*, *Trondheim* **1**, 401–404. Measurement and prediction of the reflection coefficient of porous layers for large angles of incidence and evanescent waves.
26. J. F. Allard 1993 *Propagation of Sound in Porous Media*: *Modelling Sound Absorbing Materials*. London: Chapman & Hall.
27. J. S. Bolton and E. R. Green 1992 *Technical Report*, *Ray W. Herrick Laboratory*, *Purdue University*. Smart foams for active absorption of sound.

28. D. J. JOHNSON, J. KOPLIK and R. DASHEN 1987 *Journal of Fluid Mechanics* **176**, 379–402. Theory of dynamic permeability and tortuosity in fluid-saturated porous media.
29. Y. CHAMPOUX and J. F. ALLARD 1991 *Journal of Applied Physics* **70**, 1975–1979. Dynamic tortuosity and bulk modulus in air-saturated porous media.
30. J. F. ALLARD and Y. CHAMPOUX 1992 *Journal of the Acoustical Society of America* **91**, 3346–3353. New empirical equations for sound propagation in rigid frame fibrous materials.
31. C. CARME 1987 *Ph.D. Dissertation*, *Université d'Aix-Marseille II*. Absorption acoustique active dans les cavités.